Periodic-orbit theory of the blowout bifurcation

Yoshihiko Nagai* and Ying-Cheng Lai†
Department of Physics and Astronomy, Kansas Institute for Theoretical and Computational Science, University of Kansas, Lawrence, Kansas 66045
(Received 9 May 1997)

This paper presents a theory for characterization of the blowout bifurcation by periodic orbits. Blowout bifurcation in chaotic systems occurs when a chaotic attractor, lying in some symmetric invariant subspace, becomes transversely unstable. We present an analysis and numerical results that indicate that the bifurcation is mediated by changes in the transverse stability of *an infinite number of unstable periodic orbits embedded in the chaotic attractor*. There are two distinct groups of periodic orbits: one transversely stable and another transversely unstable. The bifurcation occurs when some properly weighted transverse eigenvalues of these two groups are balanced. Our results thus categorize the blowout bifurcation as a unique type of bifurcation that involves an infinite number of periodic orbits, in contrast to most previously known bifurcations that are mediated by only a finite number of periodic orbits. [S1063-651X(97)08610-8]

PACS number(s): 05.45.+b

I. INTRODUCTION

A central problem in the study of nonlinear dynamical systems is to understand how the asymptotic behavior alters as a system parameter changes. Qualitative changes in the system's asymptotic behavior are called *bifurcations*, whereas the critical parameter values at which the bifurcations occur are the bifurcation points. The phenomenon of bifurcation is extremely common in nonlinear systems. For instance, chaos typically arises from a nonchaotic state through a series of bifurcations and the number of bifurcations involved in the creation of chaos can be as a few as one or can be as many as infinite. Understanding various types of the bifurcations has been one of the focuses in the study of nonlinear physical systems [1]. Since almost all qualitative changes in the system's behavior are due to bifurcations, it is of paramount physical interest to characterize bifurcations in terms of fundamental quantities of the system. ''There is nothing more fundamental than to characterize a bifurcation in terms of the periodic orbits embedded in the natural dynamics of the system.'' Thus the knowledge of periodic orbits is the key to understand the bifurcation and, consequently, the key to understand the dynamics of the system.

Most known bifurcations in nonlinear dynamical systems involve only a finite number of periodic orbits. Examples include the period-doubling bifurcation [2] and the saddle-node bifurcation [1]. In a period-doubling bifurcation, a stable periodic orbit of period p becomes unstable and simultaneously a stable periodic orbit of period $2p$ is created at the bifurcation [2]. In a saddle-node bifurcation, a pair of periodic orbits, one stable and another unstable, is created as the parameter passes through the bifurcation point [1]. Other examples of bifurcations include sudden catastrophic events in chaotic systems such as crises [3] and basin boundary metamorphoses [4], which are triggered by the collision of periodic orbits, usually of low period, embedded in different dynamical invariant sets. More recently, an exotic type of basin structure was discovered in chaotic systems, that is, the basin of Wada. Wada basin boundaries are common fractal boundaries of more than two basins of attraction. It was shown in Ref. [5] that Wada basin boundaries are created by a saddle-node bifurcation on the basin boundary. A direction of intense recent investigation concerns bifurcation in dynamical systems with one or several symmetric invariant subspaces. In such systems, it was discovered that the riddling bifurcation, a bifurcation that leads to the creation of riddled basins [6], is triggered by the loss of the transverse stability of some periodic orbit, typically of low period, embedded in the chaotic attractor in the invariant subspace [7]. A common feature of all these major bifurcations is that there are only *one or a few* periodic orbits involved.

The main purpose of this paper is to present a periodic-orbit theory for a recently discovered bifurcation in chaotic systems. This is the so-called *blowout bifurcation* that occurs in systems with a simple type of symmetry (see below for a precise description). ''Our main conclusion is that the blowout bifurcation is fundamentally different from most known major bifurcations in that it involves an infinite number of periodic orbits.'' We provide a quantitative characterization of the blowout bifurcation in terms of periodic orbits. A short account of this work has been published recently [8].

A fundamental requirement for the blowout bifurcation is symmetry. The existence of symmetry in the system's equations often leads to a low-dimensional invariant subspace in the phase space. Denote the invariant subspace by **S** and assume there is a chaotic attractor in **S**. Since **S** is invariant, initial conditions in **S** generate trajectories that remain in **S** forever. Trajectories off **S**, however, can either be attracted towards **S** or be repelled away from it, depending on a system parameter. The transition from the former to the latter situations is the *blowout bifurcation* [9]. Quantitatively, one can define an infinitesimal vector in the subspace **T** that is *transverse* to **S**. The exponential growth rate of the vector is the *transverse Lyapunov exponent*, denoted by Λ_T. When

*Electronic address: nagai@poincare.math.ukans.edu
†Also at Department of Mathematics, University of Kansas, Lawrence, KS 66045. Electronic address: lai@poincare.math.ukans.edu

Λ_T is negative, **S** attracts nearby trajectories transversely and hence the chaotic attractor in **S** is also an attractor in the full phase space. If Λ_T is positive, trajectories in the neighborhood of **S** are repelled away from it and consequently the attractor in **S** is transversely unstable and it is hence not an attractor of the full system. Blowout bifurcation occurs when Λ_T changes from negative to positive values. There are interesting physical phenomena associated with the blowout bifurcation. For example, near the bifurcation point where Λ_T is slightly negative, if there are attractors off **S** in the phase space, then typically the basin of the chaotic attractor in **S** is riddled with arbitrarily small holes that belong to the basin of the other attractors [6]. When Λ_T is slightly positive, if there are no other attractors in the phase space, the dynamics in the transverse subspace **T** exhibits an extreme type of temporally intermittent bursting behavior, the *on-off intermittency* [10]. Recent studies have also revealed that a blowout bifurcation can lead to symmetry breaking in chaotic systems [11].

In this paper, we present a *quantitative characterization* of the blowout bifurcation by unstable periodic orbits embedded in the chaotic attractor in the invariant subspace **S** [12]. In particular, we argue that near the bifurcation, there exist two groups of unstable periodic orbits, denoted by Σ_s and Σ_u, each having an infinite number of members, one transversely stable and another transversely unstable, respectively. The sign of the transverse Lyapunov exponent Λ_T of a typical chaotic trajectory in **S** is determined by the relative weights of Σ_s and Σ_u: Λ_T is negative (positive) when Σ_s (Σ_u) weighs over Σ_u (Σ_s) (see Sec. II for details). At the bifurcation, the weights of Σ_s and Σ_u are balanced. In contrast to most known bifurcations in chaotic systems that usually involve only one or a few periodic orbits [2–5,7], a blowout bifurcation is induced by changes in the transverse stability of *an infinite number of unstable periodic orbits*. The number $\overline{N_p}$ of the unstable periodic orbits of period p that change transverse stability in an arbitrarily small neighborhood about the bifurcation point grows as $\overline{N_p} \sim e^{h_T p}$, where h_T is the topological entropy of the chaotic attractor in **S**.

The rest of the paper is organized as follows. In Sec. II, we introduce our periodic-orbit theory for the blowout bifurcation. In Sec. III, we present numerical examples with both one-dimensional and two-dimensional, hyperbolic and nonhyperbolic, chaotic dynamics in the invariant subspace. In Sec. IV, we present discussions. A description of numerical algorithms for computing periodic orbits in our numerical examples is in the Appendixes.

II. THEORY

The basic ingredients for a system to exhibit a blowout bifurcation are the following [9,13,14]: (i) the phase space contains an invariant subspace, (ii) there is a chaotic attractor in the invariant subspace, and (iii) the chaotic dynamics in the invariant subspace is coupled to the dynamics in the transverse subspace. We thus consider the following class of N-dimensional discrete dynamical systems that capture the above three features:

$$\mathbf{x}_{n+1} = \mathbf{f}(\mathbf{x}_n),$$

$$\mathbf{y}_{n+1} = F(\mathbf{x}_n, \alpha)\mathbf{G}(y_n), \tag{1}$$

where $\mathbf{x} \in \mathbb{R}^{N_S}$ ($N_S \geq 1$), $y \in \mathbb{R}^{N_T}$ ($N_T \geq 1$), $N_S + N_T = N$, and α is the bifurcation parameter. The function $\mathbf{G}(\mathbf{y})$ satisfies $\mathbf{G}(\mathbf{0}) = \mathbf{0}$, so that $\mathbf{y} = \mathbf{0}$ is the invariant subspace **S**. The dynamics in **S** is governed by the map $\mathbf{f}(\mathbf{x})$, which has a chaotic attractor. The largest transverse Lyapunov exponent Λ_T for a typical trajectory on the chaotic attractor in **S** is given by

$$\Lambda_T = \lim_{L\to\infty} \frac{1}{L} \sum_{n=1}^{L} \ln \left| F(\mathbf{x}_n, \alpha)\mathbf{D}\mathbf{G}(\mathbf{y}_n) \right|_{\mathbf{y}_n = \mathbf{0}} \cdot \mathbf{u}|, \tag{2}$$

where $\mathbf{u}$ is a randomly chosen vector in $\mathbb{R}^{N_T}$. Assume that a blowout bifurcation occurs at α_c. That is, as the parameter α passes through α_c, Λ_T crosses zero from the negative side.

We now *qualitatively* describe how periodic orbits are involved in the blowout bifurcation. The key observation is that the chaotic attractor in **S** has embedded within itself an infinite number of unstable periodic orbits and a blowout bifurcation is caused by the change in the transverse stability of a *typical trajectory with respect to the natural measure* on the chaotic attractor in **S**. Such a trajectory visits the neighborhoods of the infinite number of unstable periodic orbits from time to time. The periodic orbits embedded in the chaotic attractor are *atypical* in the sense that they form a Lebesgue measure zero set. With probability one, randomly chosen initial conditions do not yield trajectories that exist on unstable periodic orbits. Invariant measures produced by unstable periodic orbits are thus atypical, and there is an infinite number of such atypical invariant measures embedded in a chaotic attractor. The natural measure, on the other hand, is typical in the sense that it is generated by a trajectory originated from any one of the randomly chosen initial conditions in the basin of attraction. In this sense, chaos can be considered as being organized with respect to the unstable periodic orbits [15]. In systems that exhibit a blowout bifurcation, the transverse stability of a typical trajectory is thus determined by the transverse stability of the infinite number of unstable periodic orbits that the trajectory visits in different time intervals. Among these periodic orbits, some are transversely stable and the others are transversely unstable near the bifurcation. If ''more'' periodic orbits are transversely stable (unstable), the typical trajectory is transversely stable (unstable). The bifurcation occurs when there are approximately equal numbers of the transversely stable and the transversely unstable periodic orbits so that on average the typical trajectory experiences an exactly equal amount of attraction towards and repulsion away from the invariant subspace **S**. Since there is an infinite number of periodic orbits in the chaotic attractor, the blowout bifurcation must then involve the change in the transverse stability of an infinite number of periodic orbits.

To *quantitatively* characterize the blowout bifurcation in terms of unstable periodic orbits, it is necessary to define the transverse stability of the periodic orbits. Let $\mathbf{x}_1(j), \mathbf{x}_2(j), \ldots, \mathbf{x}_p(j)$ be the jth period-p orbit embedded in the chaotic attractor in **S**, where $j = 1,2,\ldots,N_p$, N_p is the total number of the period-p orbits, and

$$\mathbf{x}_{n+1}(j)=\mathbf{f}(\mathbf{x}_n(j)), \quad n=1,2,\ldots,p-1$$

$$\mathbf{f}(\mathbf{x}_p(j))=\mathbf{x}_1(j). \tag{3}$$

We define the following transverse Lyapunov exponent for this periodic orbit:

$$\lambda_p^T(j)=\frac{1}{p}\sum_{n=1}^{p} \ln|\mathbf{F}(x_n,\alpha)\mathbf{DG}(\mathbf{0})|_{\mathbf{x}_n=\mathbf{x}_n(j)}. \tag{4}$$

If $\lambda_p^T(j)<0$ (>0), this period-p orbit is transversely stable (unstable). Thus all the period-p orbits can be divided into two groups: one transversely stable and another transversely unstable. We then introduce the period-p transversely stable and unstable weights

$$\Lambda_p^s(\alpha)=\sum_{j=1}^{N_p^s} \mu_p(j)\lambda_p^T(j)\Big|_{\lambda_p^T(j)<0},$$
$$\Lambda_p^u(\alpha)=\sum_{j=1}^{N_p^u} \mu_p(j)\lambda_p^T(j)\Big|_{\lambda_p^T(j)>0}, \tag{5}$$

where N_p^s and N_p^u are the numbers of the transversely stable and unstable period-p orbits, respectively, $N_p^s+N_p^u=N_p$, and $\mu_p(j)$ is the natural measure of a typical trajectory in the neighborhood of the jth period-p orbit.

To compute the transversely stable and unstable weights in Eq. (5), it is necessary to compute the natural measure of a typical trajectory contained in the small neighborhood of each periodic orbit. This measure is roughly the probability that the typical trajectory visits the neigborhood of the periodic orbit. Intuitively, the probability is smaller if the periodic orbit is more unstable or the magnitude of its unstable eigenvalue is larger. Thus we expect the probability of a visit to be inversely proportional to the largest unstable eigenvalue of the periodic orbit. To be precise, we make use of the results in Refs. [16,17], which relate the natural measure to the infinite number of *atypical* measures associated with all unstable periodic orbits [16]. For the map $\mathbf{f}(\mathbf{x})$, let $\mathbf{x}_p(j)$ be the jth fixed point of the p-times iterated map, i.e., $\mathbf{f}^p(\mathbf{x}_p(j))=\mathbf{x}_p(j)$. Thus each $\mathbf{x}_p(j)$ is on a periodic orbit whose period is either p or factors of p. The natural measure of a chaotic attractor in a phase space region Ω is given by

$$\mu(\Omega)=\lim_{p\to\infty}\sum_{\mathbf{x}_p(j)\in\Omega}\frac{1}{L_1(\mathbf{x}_p(j))}, \tag{6}$$

where $L_1(\mathbf{x}_p(j))$ is the magnitude of the expanding eigenvalue of the Jacobian matrix $\mathbf{Df}^p(\mathbf{x})$ evaluated at $\mathbf{x}_p(j)$ and the summation is taken over all fixed points of $\mathbf{f}^p(\mathbf{x})$ in Ω. If the phase-space region Ω contains the entire chaotic attractor, then

$$\lim_{p\to\infty}\sum_{\mathbf{x}_p(j)\in\Omega}\frac{1}{L_1(\mathbf{x}_p(j))}=1. \tag{7}$$

Although Eq. (6) was derived under the condition that the map $\mathbf{f}(\mathbf{x})$ be hyperbolic [18], it was conjectured [16] that Eq. (6) holds for nonhyperbolic maps as well, which was supported by strong numerical evidence [17]. For periodic orbits of finite period p (large), the summation in Eq. (7) is approximately unity but not exactly. Thus we make use of the following normalized natural measure associated with the jth period-p periodic orbit:

$$\mu_p(j)\equiv\frac{1/L_1(\mathbf{x}_p(j),p)}{\sum_{j=1}^{N_p}[1/L_1(\mathbf{x}_p(j),p)]}. \tag{8}$$

Equation (7) indicates that in the limit $p\to\infty$, the natural measure of the chaotic attractor is precisely characterized by the probabilities of a visit to all the periodic orbits of period p. At the blowout bifurcation point where the transverse Lyapunov exponent of a typical trajectory on the chaotic attractor becomes zero, we expect that the weights of the transversely stable and transversely unstable periodic orbits are balanced precisely. Setting

$$\Lambda^{s,u}(\alpha)=\lim_{p\to\infty}\Lambda_p^{s,u}(\alpha), \tag{9}$$

we formulate the following periodic-orbit theory of the blowout bifurcation:

$$\Lambda^u(\alpha)<|\Lambda^s(\alpha)| \quad \text{for } \alpha<\alpha_c,$$
$$\Lambda^u(\alpha)>|\Lambda^s(\alpha)| \quad \text{for } \alpha>\alpha_c, \tag{10}$$
$$\Lambda^u(\alpha)=|\Lambda^s(\alpha)| \quad \text{for } \alpha=\alpha_c.$$

III. NUMERICAL CONFIRMATION

To confirm our theory, it is necessary to find systems for which all the periodic orbits embedded in the chaotic attractor in the invariant subspace **S** can be computed. We have thus selected the following maps in **S**: (i) the one-dimensional doubling transformation, (ii) the two-dimensional Kaplan-Yorke map [19], and (iii) the two-dimensional Hénon map [20].

A. The doubling transformation

The full system is the two-dimensional version of Eq. (1) with $F(x_n,\alpha)=\alpha x_n$,

$$x_{n+1}=f(x_n)=2x_n(\mathrm{mod}1),$$
$$y_{n+1}=\alpha x_n g(y_n), \tag{11}$$

where the x dynamics is the doubling transformation that generates a chaotic attractor with uniform invariant density $\rho(x)=1$ for $x\in[0,1]$ and the function $g(y)$ satisfies $g(0)=0$ and $g'(0)=\mathrm{const}$ (which we chose to be 1). The Lyapunov exponent of the doubling transformation is $\ln 2$. There are many choices for $g(y)$, e.g., $g(y)=y(1-y)$ (the logistic function) and $g(y)=(1/2\pi)\sin(2\pi y)$ [11]. The transverse Lyapunov exponent of Eq. (11) is

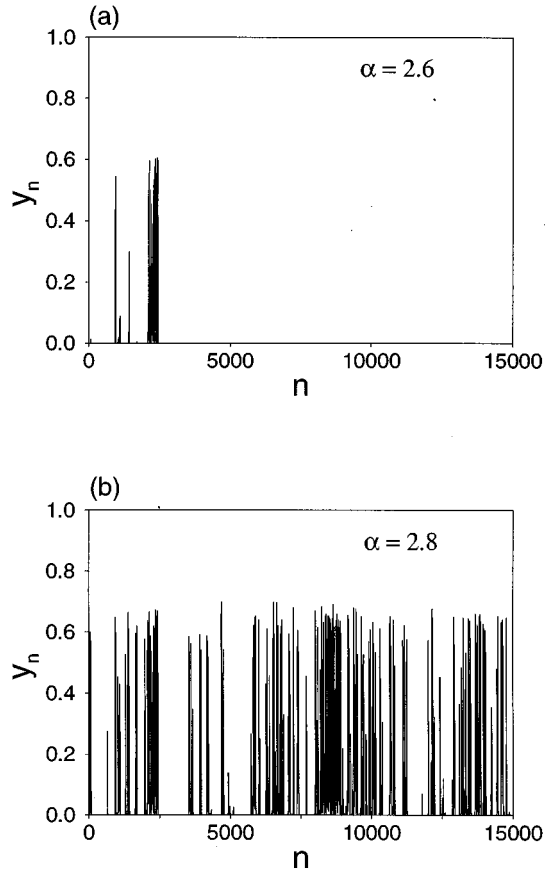

FIG. 1. For the model (11), (a) time series y_n at $\alpha=2.6$ (before the blowout bifurcation that occurs at $\alpha_c=e$) and (b) time series y_n at $\alpha=2.8$ (after the blowout bifurcation).

$$\Lambda_T(\alpha)=\lim_{n\to\infty}\frac{1}{n}\sum_{j=1}^{n}\ln(\alpha x_j)=\int_0^1\ln(\alpha x)\rho(x)dx=\ln\alpha-1. \tag{12}$$

A blowout bifurcation thus occurs at $\alpha_c=e=2.718\,28\ldots$, where $\Lambda_T<0$ for $\alpha<\alpha_c$ and $\Lambda_T\geqslant 0$ for $\alpha\geqslant\alpha_c$. The behaviors of a typical trajectory of Eq. (11) are qualitatively different for values of α before and after the bifurcation. For $\alpha<\alpha_c$, a typical trajectory has $\lim_{n\to\infty}y_n=0$ if there are no other attractors in the two-dimensional phase space (x,y) except the one generated by the doubling transformation in $y=0$, as shown in Fig. 1(a), where y_n versus n is plotted, $\alpha=2.6<e$, and $g(x)=(1/2\pi)\sin(2\pi y)$. For $\alpha>\alpha_c$, a typical trajectory no longer asymptotically approaches $y=0$ but instead, it can burst away from $y=0$ intermittently, as shown in Fig. 1(b), where $\alpha=2.8>e$. Figure 1(b) represents a typical situation of on-off intermittency [10].

The unstable periodic orbits embedded in the chaotic attractor of the doubling transformation can be computed explicitly (see Appendix A). The eigenvalue of a period-p orbit is 2^p and, hence, the normalized natural measure contained in an arbitrarily small neighborhood of the orbit is identical for all period-p (or factors of p) orbits [Eq. (8)]. We thus write $\mu_p(j)=\mu_p$. The stable and unstable weights in Eq. (5) become

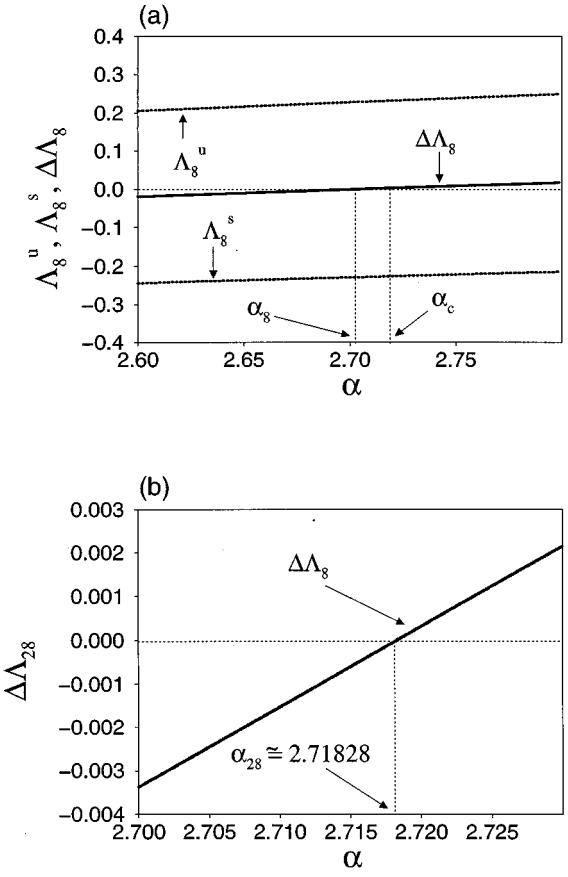

FIG. 2. For the model (11), (a) for all the period-8 orbits, $\Lambda_8^s(\alpha)$ (the transversely stable weight), $\Lambda_8^u(\alpha)$ (the transversely unstable weight), and $\Delta\Lambda_8(\alpha)\equiv\Lambda_8^u(\alpha)-|\Lambda_8^s(\alpha)|$ versus α near the blowout bifurcation point. We see that $\Delta\Lambda_8(\alpha)$ crosses zero at $\alpha_8\approx 2.702\,28$ ($|\alpha_8-\alpha_c|\approx 0.016$). (b) For all the period-28 orbits, $\Delta\Lambda_2 8(\alpha)$ versus α. Now $|\alpha_{28}-\alpha_c|\sim 10^{-8}$.

$$\Lambda_p^s(\alpha)=\mu_p\sum_{j=1}^{N_p^s}\lambda_p^T(j)|_{\lambda_p^T(j)<0},$$
$$\Lambda_p^u(\alpha)=\mu_p\sum_{j=1}^{N_p^u}\lambda_p^T(j)|_{\lambda_p^T(j)>0}. \tag{13}$$

To verify our main result, Eq. (10), we choose a small parameter interval around the blowout bifurcation point $\alpha_c=e$ and evenly distribute a large number of parameter values α in this interval. For each α value, we compute $\Lambda_p^s(\alpha)$ and $\Lambda_p^u(\alpha)$ for all the distinct periodic orbits up to period 28. (For $p=28$, there are 9 586 395 distinct periodic orbits.) Figure 2(a) shows the period-8 weights $\Lambda_8^s(\alpha)$ and $\Lambda_8^u(\alpha)$ (dotted lines) versus α for $\alpha\in[2.6,2.8]$. The solid line in Fig. 2(a) is $\Delta\Lambda_8(\alpha)\equiv\Lambda_8^u(\alpha)-|\Lambda_8^s(\alpha)|$ versus α. We obtain $\alpha_8\approx 2.702\,28$, where α_8 is the critical parameter value at which $\Delta\Lambda_8(\alpha_8)=0$. The difference between α_8 and the theoretical bifurcation point α_c is $\Delta\alpha_8\equiv|\alpha_8-\alpha_c|\approx 0.016$, which is rather large. However, as we examine periodic orbits of higher periods, the difference $|\alpha_p-\alpha_c|$ decreases rapidly. Figure 2(b) shows $\Delta\Lambda_{28}(\alpha)$ versus α for $\alpha\in[2.70,2.73]$. We obtain $\alpha_{28}\approx\alpha_c-2.31\times10^{-8}$ so that $\Delta\alpha_{28}\sim 10^{-8}$. Fig-

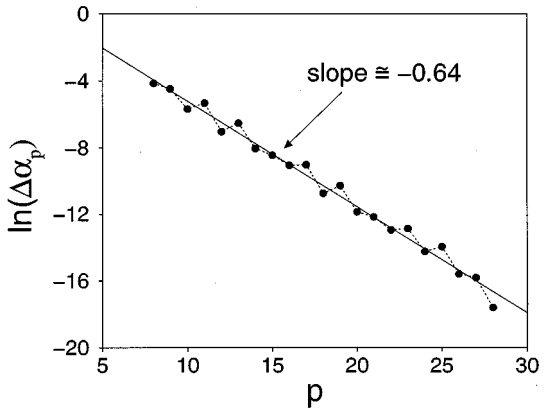

FIG. 3. For the model (11), $\ln(\Delta\alpha_p)$ versus p. It can be seen that $\ln(\Delta\alpha_p)\sim e^{-h_T p}$, where $h_T=\ln 2$ is the topological entropy of the doubling transformation attractor.

ure 3 shows, on a semilogarithmic scale, the error $\Delta\alpha_p \equiv|\alpha_p-\alpha_c|$ versus the period p for $p\in[8,28]$. The data can be roughly fitted by a straight line with a slope of about -0.64, indicating the exponential scaling law for $\Delta\alpha_p$,

$$\Delta\alpha_p\sim e^{-0.64p}, \tag{14}$$

where the scaling exponent 0.64 is approximately the topological entropy ($h_T=\ln 2$) of the chaotic attractor of the doubling transformation. Thus, we expect that as the period p increases, the collective behavior of all the period-p orbits, quantitatively described by the transversely stable and unstable weights in Eq. (13), more and more precisely characterizes the blowout bifurcation.

To analytically understand the scaling law, Eq. (14), we note from Eq. (13) that $\Delta\alpha_p\sim|\Delta\Lambda_p(\alpha_c)|\sim\Delta\mu(p)$, where $\Delta\mu(p)$ is the difference between the natural measure computed from a typical trajectory and that computed from all the period-p orbits. To estimate $\Delta\mu(p)$, we divide the unit interval in which the chaotic attractor lies into N bins so that the size of each bin is $\epsilon=1/N$. The natural measure contained in each bin is ϵ because it is uniform in the unit interval. There are $(2^p\pm1)/N$ fixed points of the pth-iterated map in each bin. Since all periodic orbits of period p of the doubling transformation have the same eigenvalue 2^p, we obtain $\mu(p)=[(2^p\pm1)/N]/2^p=\epsilon(1\pm2^{-p})$. Thus we have $\Delta\mu(p)=|\mu(p)-\epsilon|\sim 2^{-p}=\exp(-p\ln 2)$, which gives Eq. (14).

As we have argued in Sec. II, the fundamental characteristic that distinguishes a blowout bifurcation from other known bifurcations is that it involves the change in the transverse stabilities of an infinite number of periodic orbits. To verify this, we investigate the scaling with the period of the number of periodic orbits that change from being transversely stable to being transversely unstable when the bifurcation parameter α changes from slightly below to slightly above α_c. We find that this number increases exponentially with p. Figure 4 shows $\ln\overline{N_p}$ versus p for $p\in[8,28]$, where $\overline{N_p}$ is the number of periodic orbits of period p that change their transverse stabilities as α is increased from 2.70 to 2.73. The plot can be fitted by a straight line with a slope 0.62 ($\approx h_T$), indicating the scaling law,

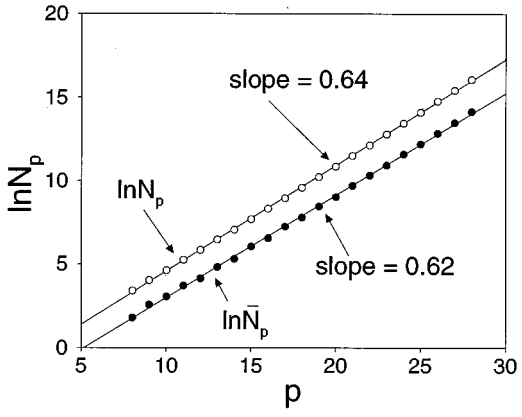

FIG. 4. For the model (11), $\ln\overline{N_p}$ versus p (closed circles), where $\overline{N_p}$ is the number of period-p orbits that changes from being transversely stable to transversely unstable when α is increased from 2.70 to 2.73. The upper curve with open circles is $\ln N_p$ versus p, where N_p is the number of all the period-p orbits. Clearly, we have $N_p\sim e^{h_T p}$ and $\overline{N_p}\sim e^{h_T p}$.

$$\overline{N_p}\sim e^{h_T p}. \tag{15}$$

As a comparison, the dotted line in Fig. 4 shows the total number N_p of distinct period-p orbits versus p (also on a semilogarithmic scale), the slope of which is an estimate of the topological entropy h_T. We see that the two plots are practically parallel, with the plot of $\ln\overline{N_p}$ versus p shifted downward. This indicates that a fraction of all the periodic orbits change their transverse stabilities near the blowout bifurcation. Reducing the range in which α changes around the bifurcation point α_c only causes a further parallel downward shift of the plot $\overline{N_p}$ versus p. Due to the scaling law, Eq. (15), there must be an infinite number of periodic orbits that change their transverse stabilities in arbitrarily small parameter intervals about the bifurcation point. Figure 4 thus strongly supports our claim that the blowout bifurcation involves an infinite number of periodic orbits.

B. The Kaplan-Yorke map

We study the following three-dimensional version of Eq. (1) with a Kaplan-Yorke chaotic attractor in the invariant subspace $z=0$ (the x-y plane):

$$\begin{aligned} x_{n+1}&=\gamma x_n+\frac{1}{\pi}\sin(2\pi y_n),\\ y_{n+1}&=2y_n(\mathrm{mod}1),\\ z_{n+1}&=\frac{1}{2\pi}(\alpha x_n+\beta y_n)\sin(2\pi z_n), \end{aligned} \tag{16}$$

where α and β are parameters. The transverse Lyapunov exponent for a typical trajectory in the chaotic attractor in $z=0$ is

$$\Lambda_T=\lim_{n\to\infty}\frac{1}{n}\sum_{j=1}^{n}\ln|\alpha x_j+\beta y_j|.$$

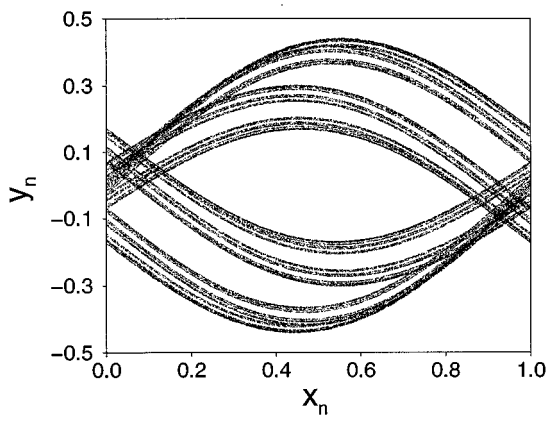

FIG. 5. Kaplan-Yorke chaotic attractor at $\gamma=0.4$. The attractor is hyperbolic.

The Kaplan-Yorke map in the x-y plane generates a hyperbolic chaotic attractor with a positive Lyapunov exponent ln2. Figure 5 shows such an attractor at $\gamma=0.4$. All periodic orbits of the Kaplan-Yorke map can be calculated explicitly (see Appendix B). The expanding eigenvalues of all the period-p orbits are 2^p. Choosing $\beta=0$ (a rather arbitrary choice), we find that $\alpha_c=2\pi$ is the blowout bifurcation point, where $\Lambda_T<0$ for $\alpha<\alpha_c$ and $\Lambda_T\geqslant 0$ for $\alpha\geqslant\alpha_c$.

Figure 6(a) shows the period-12 weights $\Lambda_{12}^s(\alpha)$ and $\Lambda_{12}^u(\alpha)$ (dotted lines) versus α for $\alpha\in[6.0,6.3]$. The solid line in Fig. 6(a) is $\Delta\Lambda_{12}(\alpha)\equiv\Lambda_{12}^u(\alpha)-|\Lambda_{12}^s(\alpha)|$ versus α. We obtain $\alpha_{12}\approx 6.3023$, the critical parameter value at which the transversely stable and unstable weights of all the period-12 orbits are balanced. The difference between α_{12} and the blowout bifurcation point α_c is $\Delta\alpha_{12}\equiv|\alpha_{12}-\alpha_c|\approx 0.0191$, which is somewhat large. This difference diminishes rapidly as the period of the periodic orbits increases. Figure 6(b) shows $\Delta\Lambda_{24}(\alpha)$ versus α. We obtain $\alpha_{24}\approx 6.283\,17$ and $\Delta\alpha_{24}\approx 7\times10^{-6}$. Figure 7(a) shows $\Delta\alpha_p\equiv|\alpha_p-\alpha_c|$ versus the period p for $p\in[11,24]$. As period p increases, $\Delta\alpha_p$ decreases exponentially with the scaling law $\Delta\alpha_p\sim e^{-0.58p}$, where the scaling exponent is again roughly ln2, the topological entropy of the Kaplan-Yorke chaotic attractor [21]. Figure 7(b) shows $\ln\overline{N_p}$ versus p for $p\in[11,24]$, where $\overline{N_p}$ is the number of period-p orbits that change from being transversely stable to being transversely unstable as α is increased from 6.25 to 6.29. We obtain the scaling law $\overline{N_p}\sim e^{0.64p}$ (the solid line). The dotted line in Fig. 7(b) is $\ln N_p$ versus p, where N_p is the total number of distinct period-p orbits. This example illustrates that the conclusion that a blowout bifurcation involves an infinite number of periodic orbits is valid for the case where the dynamics in the invariant subspace exists on a two-dimensional hyperbolic chaotic attractor.

C. The Hénon map

We now consider the situation where the chaotic dynamics in the invariant subspace is nonhyperbolic. We study the three-dimensional map

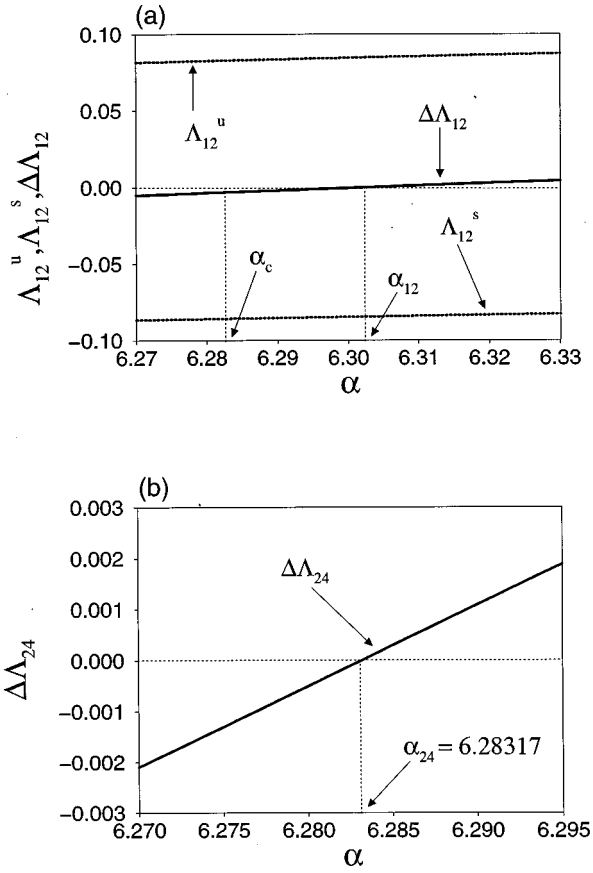

FIG. 6. For the model (16), (a) for all the period-12 orbits in the Kaplan-Yorke attractor, $\Lambda_{12}^s(\alpha)$, $\Lambda_{12}^u(\alpha)$, and $\Delta\Lambda_{12}(\alpha)\equiv\Lambda_{12}^u(\alpha)-|\Lambda_{12}^s(\alpha)|$ versus α near the blowout bifurcation point ($\alpha_c=2\pi$). We see that $\Delta\Lambda_{12}(\alpha)$ crosses zero at $a_{12}\approx 6.3023$, corresponding to $|\alpha_{12}-\alpha_c|\approx 0.0191$. (b) For all the period-24 orbits in the Kaplan-Yorke attractor, $\Delta\Lambda_{24}(\alpha)$ versus α. Now $|\alpha_{24}-\alpha_c|\approx 7\times10^{-6}$.

$$x_{n+1}=1.4-x_n^2+0.3y_n,$$

$$y_{n+1}=x_n, \tag{17}$$

$$z_{n+1}=\frac{1}{2\pi}(\alpha x_n+\beta y_n)\sin(2\pi z_n),$$

where the x-y dynamics is described by the Hénon map at a parameter setting for which there is apparently a chaotic attractor [20]. The Hénon map is one of the very few model systems for which there is a numerical algorithm to compute, in principle, all unstable periodic orbits of arbitrarily high periods [22] (see Appendix C). The Hénon attractor is also apparently nonhyperbolic because a rigorous computation of the stable and unstable manifolds [23] points towards the existence of an infinite number of tangency points of these manifolds on the attractor. All the periodic orbits up to period 31 are computed. The transversely stable and unstable weights are then computed as in Eq. (5), based on the conjecture that the unstable periodic-orbit formulation of the natural measure [Eqs. (6) and (8)] is also valid for nonhyperbolic attractors [16,17]. Choosing $\beta=0$, we find numerically

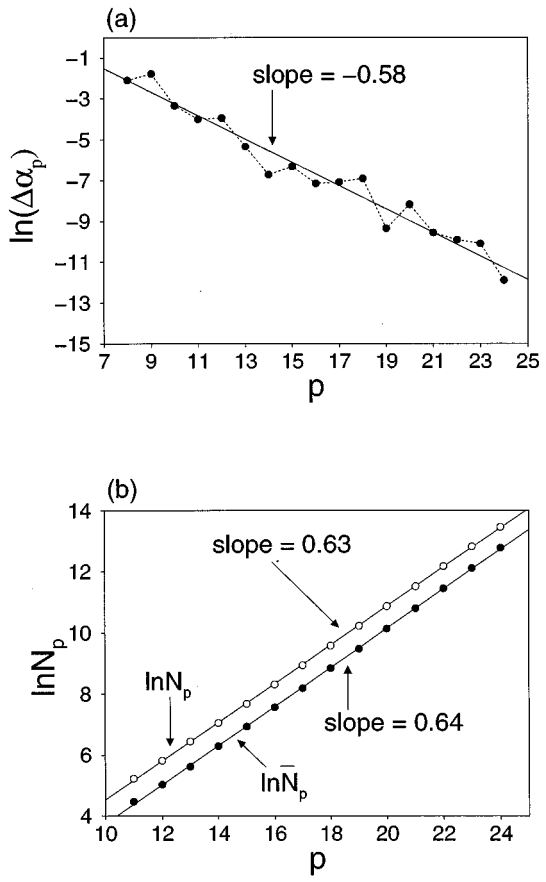

FIG. 7. For the model (16), (a) $\ln(\Delta\alpha_p)$ versus p and (b) $\ln \overline{N_p}$ versus p (filled circles), where $\overline{N_p}$ is the number of period-p orbits that changes from being transversely stable to transversely unstable when α is increased from 6.25 to 6.29. The upper curve is $\ln N_p$ versus p (open circles), where N_p is the number of all period-p orbits. We have $N_p \sim e^{h_T p}$ and $\overline{N_p} \sim e^{h_T p}$.

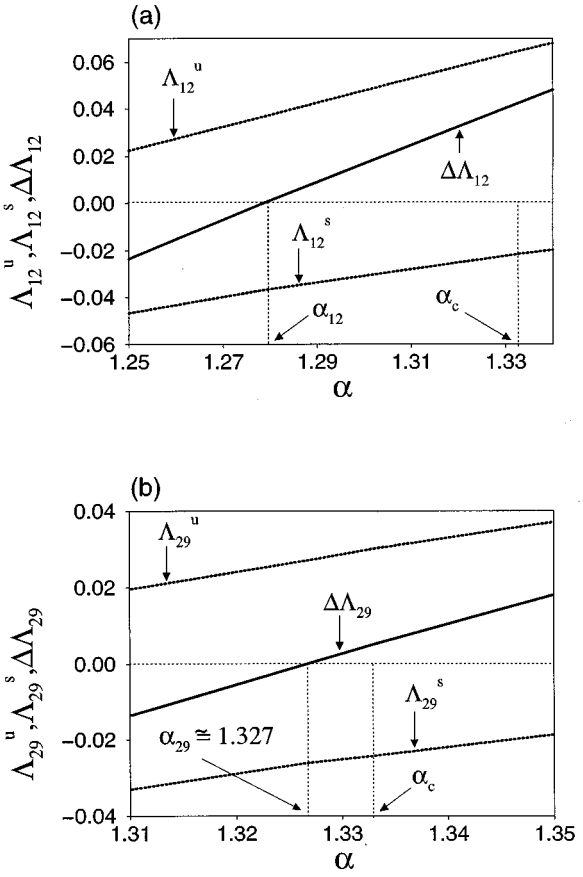

FIG. 8. For the model (17), (a) for all the period-12 orbits, $\Lambda_{12}^s(\alpha)$, $\Lambda_{12}^u(\alpha)$, and $\Delta\Lambda_{12}(\alpha) \equiv \Lambda_{12}^u(\alpha) - |\Lambda_{12}^s(\alpha)|$ versus α near the blowout bifurcation point. We see that $\Delta\Lambda_{12}(\alpha)$ crosses zero at $a_{12} \approx 1.279$ ($|\alpha_{12} - \alpha_c| \approx 0.054$). (b) For all the period-29 orbits, $\Delta\Lambda_{29}(\alpha)$ versus α. Now $|\alpha_{29} - \alpha_c| \approx 6 \times 10^{-3}$.

that a blowout bifurcation occurs at $\alpha_c \approx 1.333$, where $\Lambda_T < 0$ for $\alpha < \alpha_c$ and $\Lambda_T \geq 0$ for $\alpha \geq \alpha_c$.

Figure 8(a) shows the period-12 weights $\Lambda_{12}^s(\alpha)$ and $\Lambda_{12}^u(\alpha)$ (dotted lines) versus α for $\alpha \in [1.25, 1.35]$. The solid line in Fig. 8(a) is $\Delta\Lambda_{12}(\alpha) \equiv \Lambda_{12}^u(\alpha) - |\Lambda_{12}^s(\alpha)|$ versus α. We obtain $\alpha_{12} \approx 1.279$, the critical parameter value at which $\Delta\Lambda_{12}(\alpha) = 0$. The difference between α_{12} and bifurcation point α_c is $\Delta\alpha_{12} \equiv |\alpha_{12} - \alpha_c| \approx 0.054$. Figure 8(b) shows $\Delta\Lambda_{29}(\alpha)$ versus α for $\alpha \in [1.31, 1.35]$. We obtain $\alpha_{29} \approx 1.327$ so that $\Delta\alpha_{29} \approx 6 \times 10^{-3}$. Figure 9(a) shows the error $\Delta\alpha_p \equiv |\alpha_p - \alpha_c|$ versus the period p for $p \in [10, 31]$ on a semilogarithmic scale. The data can be roughly fitted by a straight line with a slope of about -0.11, indicating the scaling law

$$\Delta\alpha_p \sim e^{-0.11p}. \tag{18}$$

Similar to the cases of the doubling transformation and the Kaplan-Yorke map, we find that the number of the periodic orbits that change their transverse stabilities in the vicinity of α_c increases exponentially with the period, as shown in Fig. 9(b), where $\ln \overline{N_p}$ versus p is plotted for $p \in [15, 31]$ and $\overline{N_p}$ is the number of period-p orbits that change their transverse stabilities as α is increased from 1.31 to 1.35. We obtain $\overline{N_p} \sim e^{0.45p}$ (the solid line). In Fig. 9(b) the dotted line is the total number N_p of all distinct period-p orbit N_p versus p plotted on a semilogarithmic scale. Figure 9(b) thus indicates that even when the chaotic dynamics in the invariant subspace in nonhyperbolic, an infinite number of periodic orbits change their transverse stabilities about the blowout bifurcation. The somewhat large fluctuation in Fig. 9(a) is partly due to nonhyperbolicity of the Hénon attractor. It is also clear that nonhyperbolicity causes the scaling exponent in Eq. (18) to deviate from the topological entropy ($h_T \approx 0.43$ for the Hénon attractor), but nonetheless the scaling law is still exponential.

The three numerical examples we have studied above apparently all yield the same conclusion: ''A blowout bifurcation is mediated by a change in the transverse stability of an infinite number of unstable periodic orbits embedded in the chaotic attractor in the invariant subspace.''

IV. DISCUSSION

The main conclusion of this paper is that from the standpoint of periodic orbits, blowout bifurcation is fundamentally different from most known bifurcations that involve a finite number of periodic orbits. A blowout bifurcation involves

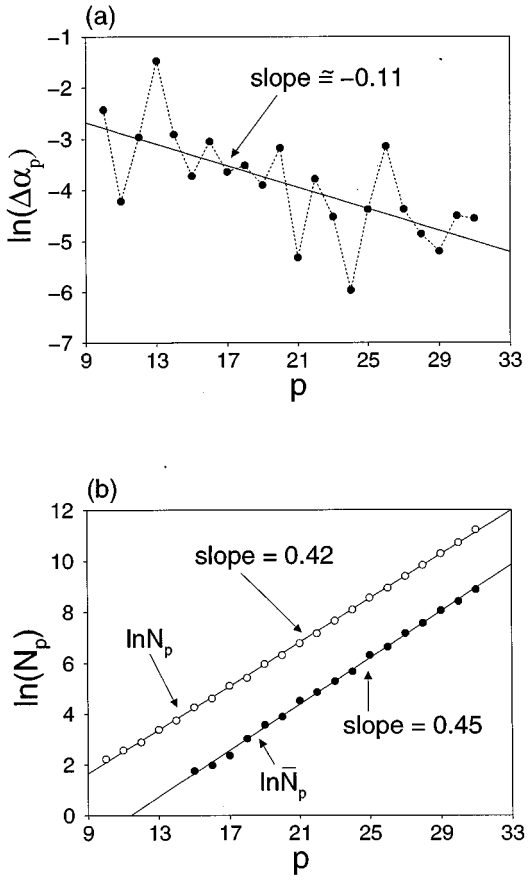

FIG. 9. For the model (17), (a) $\ln(\Delta\alpha_p)$ versus p and (b) $\ln \overline{N_p}$ versus p (filled circles), where $\overline{N_p}$ is the number of period-p orbits that changes from being transversely stable to transversely unstable when α is increased from 1.31 to 1.35. The upper curve is $\ln N_p$ versus p (open circles). We have $N_p \sim e^{h_T p}$ and $\overline{N_p} \sim e^{h_T p}$.

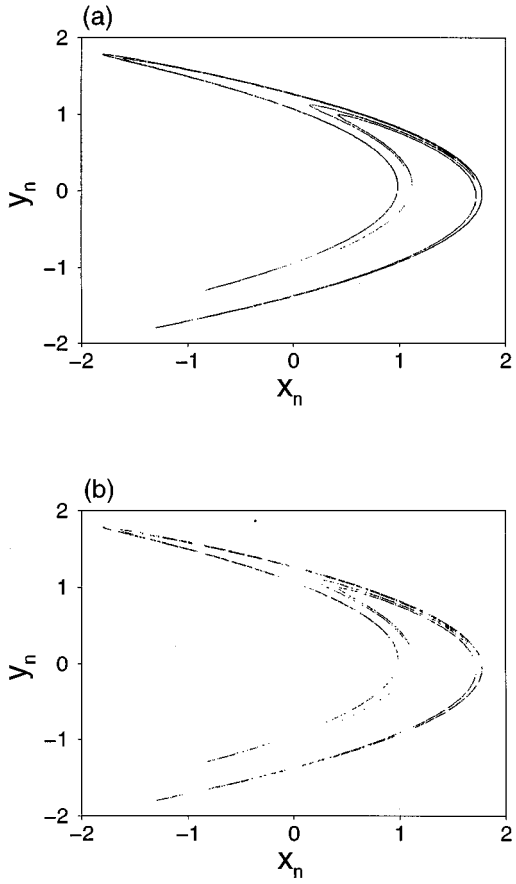

FIG. 10. For the model (17) at $\alpha = 1.23$ (before the blowout bifurcation), (a) the locations of all the transversely stable periodic orbits of period 23 and (b) the locations of all the transversely unstable periodic orbits of period 23.

two distinct groups of unstable periodic orbits with different numbers of unstable directions. Take, for instance, the three-dimensional map, Eq. (17). The two groups are the transversely stable and unstable ones: Periodic orbits in the former group have one unstable direction, while those in the latter group have two. Before (after) the bifurcation when the transverse Lyapunov exponent of a typical trajectory on the chaotic attractor is negative (positive), there are ''more'' members in the transversely stable (unstable) group, quantitatively described by the weights in Eq. (5). To visualize these two groups of unstable periodic orbits, we plot, for Eq. (17), the locations of all the transversely stable and unstable periodic orbits of period 23, as shown in Figs. 10(a) and 10(b), respectively, for $\alpha = 1.23 < \alpha_c$ (before the blowout bifurcation). Clearly, there are more transversely stable periodic orbits. After the bifurcation, there are more transversely unstable periodic orbits, as shown in Figs. 11(a) and 11(b) for $\alpha = 1.4 > \alpha_c$. In fact, the sets of all the transversely stable and unstable periodic orbits exist on nonattracting chaotic saddles embedded in the chaotic attractor. As the parameter increases towards the bifurcation point, an infinite number of periodic orbits belonging to the transversely stable group switch continuously to the transversely unstable group. The bifurcation is triggered when the dynamical weights [Eq. (5)] of the two groups are balanced *exactly*. Since there is an infinite number of unstable periodic orbits embedded in the chaotic attractor, as quantified by a positive value of the topological entropy, a subset of an infinite number of periodic orbits changes their numbers of unstable directions at the blowout bifurcation. An implication of this scenario is that the bifurcation occurs smoothly as a parameter changes, as quantified by the smooth change of the transverse Lyapunov exponent through the bifurcation point [9,13,14]. We mention that the class of systems investigated in this paper, i.e., chaotic systems with an invariant subspace, mathematically described by Eq. (1), are of physical interest. These occur naturally in systems with spatial symmetry and in systems such as coupled oscillators that model a large variety of phenomena in physics, chemistry, biology, and ecology [24,13,25].

In order to characterize the blowout bifurcation by unstable periodic orbits, it is necessary to compute the locations of all periodic orbits up to reasonably high periods, which is in general a difficult task. However, we believe that our results are general because our model, Eq. (1) captures the essential features of the blowout bifurcation [9,13,14] and our numerical examples include both one-dimensional and two-dimensional, hyperbolic and nonhyperbolic, chaotic dynamics in the invariant subspace. In particular, the Hénon map has been a paradigm in the study of chaotic systems.

Finally, we stress that in this paper, although the periodic-

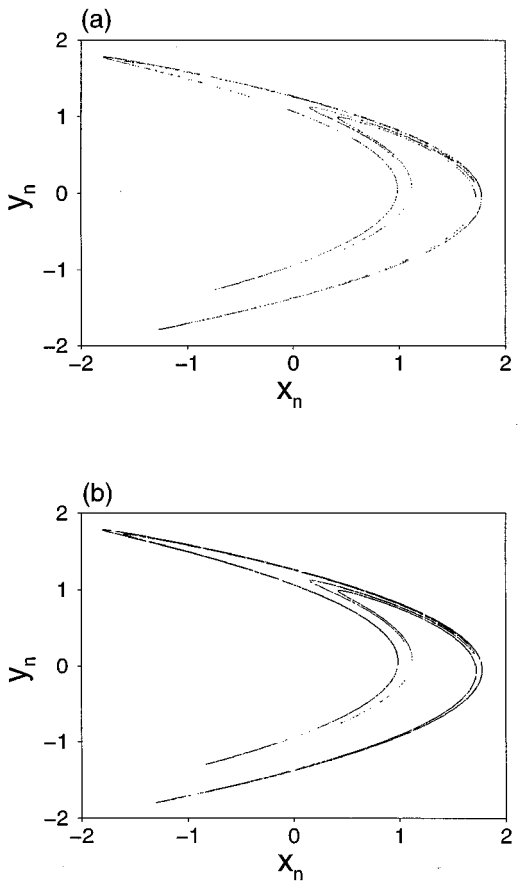

FIG. 11. For the model (17) at $\alpha=1.4$ (after the blowout bifurcation), (a) the locations of all the transversely stable periodic orbits of period 23 and (b) the locations of all the transversely unstable periodic orbits of period 23.

orbit theory of the blowout bifurcation was confirmed numerically by utilizing exclusively discrete maps, we expect the theory to be valid for continuous chaotic systems as well. Our confidence relies on the well-known fact that the dynamics of a continuous flow can be faithfully represented by that of a discrete map on a Poincaré surface of section [26]. It has then become possible for our theory to be tested because certain discrete maps (not many of them though) allow for the computation of *all* periodic orbits up to some reasonably high periods. As such, our numerical results can be regarded as an *indirect* check for the blowout bifurcation in continuous dynamical systems. It would certainly be interesting to be able to check directly the applicability of our theory for continuous systems, but this demands a direct computation of *all* unstable periodic orbits up to high periods for continuous flows. While certain periodic orbits can be computed for continuous flows such as the Lorenz system [27], at present we are not aware of any numerical procedure that allows for a *systematic* computation of all periodic orbits from a continuous system.

ACKNOWLEDGMENTS

We thank T. Tél, C. Grebogi, and P. Gaspard for valuable discussions. This work was sponsored by AFOSR under Grant No. F49620-96-1-0066, by NSF under Grant No. DMS-962659, and by the University of Kansas.

APPENDIX A: PERIODIC ORBITS OF THE DOUBLING TRANSFORMATION

The locations of the periodic orbits of the doubling transformation can be obtained explicitly. At each iteration, the map has two line segments of slope 2 in the unit square of the plane x_{n+1} versus x_n. The pth-iterated map has 2^p line segments in the unit square. Fixed points of the pth-iterated map, which contain all periodic orbits of period p or factors of p, are located at cross points of these 2^p line segments with the line $x_{n+1}=x_n$. Thus we have the following set of points that belong to different periodic orbits of period p or factors of p:

$$x_p(j)=\frac{j}{2^p-1}, \quad j=1,3,5,\ldots,2^{p-1}-1. \tag{A1}$$

Starting with one such point, one can obtain the remaining $p-1$ points on the orbit by iterating the doubling transformation map. For example, for $p=4$, we have

$$\begin{aligned} x_4(1)&=\tfrac{1}{15}\rightarrow\tfrac{2}{15}\rightarrow\tfrac{4}{15}\rightarrow\tfrac{8}{15},\\ x_4(3)&=\tfrac{3}{15}\rightarrow\tfrac{6}{15}\rightarrow\tfrac{12}{15}\rightarrow\tfrac{9}{15},\\ x_4(5)&=\tfrac{5}{15}\rightarrow\tfrac{10}{15}\rightarrow\tfrac{5}{15}\rightarrow\tfrac{10}{15},\\ x_4(7)&=\tfrac{7}{15}\rightarrow\tfrac{14}{15}\rightarrow\tfrac{13}{15}\rightarrow\tfrac{11}{15}, \end{aligned} \tag{A2}$$

where an arrow denotes doubling transformation.

APPENDIX B: PERIODIC ORBITS OF THE KAPLAN-YORKE MAP

The y dynamics in the Kaplan-Yorke map is the doubling transformation. Thus the y coordinates of the locations of the periodic orbits are the same as these in Appendix A. The x coordinates of the jth period-p orbit can be computed by noting that

$$\begin{aligned} x_{p+1}(j)=\gamma^p x_1+\frac{1}{\pi}\{&\gamma^{p-1}\sin[2\pi y_p^1(j)]\\ &+\gamma^{p-2}\sin[2\pi y_p^2(j)]+\cdots+\sin[2\pi y_p^p(j)]\}. \end{aligned} \tag{B1}$$

Setting $x_{p+1}=x_1$, we obtain the x coordinate of one point on the jth periodic orbit of period p,

$$x_p^1(j)=\frac{1}{\pi(1-\gamma^p)}\sum_{i=1}^{p}\gamma^{p-i}\sin[2\pi y_p^i(j)]. \tag{B2}$$

The remaining $p-1$ x coordinates of the periodic orbit can be obtained by either iterating the map or rearranging the order of summation in Eq. (B2).

APPENDIX C: PERIODIC ORBITS OF THE HÉNON MAP

We rewrite the Hénon map in the form

$$x_{n+1}=a-x_n^2+bx_{n-1}. \tag{C1}$$

Biham and Wenzel introduced a numerical technique to compute all the unstable periodic orbits of the Hénon map [22]. The idea is to construct the following Hamiltonian function from the map:

$$H=\frac{1}{2}\sum_n \frac{1}{b^n}\left(\frac{dx_n}{dt}\right)^2+\sum_n (-b)^{-n}\left[x_n(x_{n+1}-x_{n-1}) -\left(\frac{1}{b}+1\right)\left(ax_n-\frac{1}{3}x_n^3\right)\right]. \tag{C2}$$

The locations of the periodic orbits correspond to the stable minima on the constant energy surface. A period-p orbit is thus computed by solving the set of first-order coupled differential equations

$$\frac{dx_n}{dt}=S_nF_n=S_n(-b)^{-n}(b^{-1}+1)(-x_{n+1}+a-x_n^2 +bx_{n-1}), \quad n=1,\ldots,p, \tag{C3}$$

where $S_n=\pm 1$ and $x_{p+1}=x_1$. There are 2^p combinations of S_n's. For each combination, a randomly chosen initial condition is utilized to solve Eq. (C3). Converging solutions (x_i's, $i=1,\ldots,p$) are taken to be the locations of a periodic orbit of period p. Choosing different combinations of S_n's yields different period-p orbits, provided that the solution to Eq. (C3) converges. Diverging solutions to Eq. (C3) are disregarded. This method has proven to be very successful in computing all periodic orbits of the Hénon map up to reasonably high periods.

[1] E. Ott, *Chaos in Dynamical Systems* (Cambridge University Press, Cambridge, 1993); K. T. Alligood, T. Saure, and J. A. Yorke, *Chaos: An Introduction to Dynamical Systems* (Springer-Verlag, New York, 1996).

[2] M. J. Feigenbaum, J. Stat. Phys. **19**, 25 (1978).

[3] A crisis is triggered by the collision of a periodic orbit, usually of low period, embedded in the chaotic attractor, either with the basin boundary (boundary crisis) or with a nonattracting chaotic saddle (interior crisis). See C. Grebogi, E. Ott, and J. A. Yorke, Phys. Rev. Lett. **48**, 1507 (1982); Physica D **7**, 181 (1983).

[4] Basin boundaries in nonlinear systems with multiple coexisting attractors can undergo metamorphoses when an unstable periodic orbit on the boundary collides with a nonattracting chaotic saddle. See C. Grebogi, E. Ott, and J. A. Yorke, Phys. Rev. Lett. **56**, 1011 (1986); Physica D **24**, 243 (1987).

[5] H. E. Nusse, E. Ott, and J. A. Yorke, Phys. Rev. Lett. **75**, 2482 (1995); H. E. Nusse and J. A. Yorke, Physica D **90**, 242 (1996).

[6] ''Riddling'' means that for every point in the basin of the chaotic attractor in the invariant subspace there are points arbitrarily nearby that belong to the basins of other attractors. See, for example, J. C. Alexander, J. A. Yorke, Z. You, and I. Kan, Int. J. Bifurcation Chaos **2**, 795 (1992); I. Kan, Bull. Am. Math. Soc. **31**, 68 (1994); E. Ott, J. C. Alexander, I. Kan, J. C. Sommerer, and J. A. Yorke, Physica D **76**, 384 (1994); Y.-C. Lai and C. Grebogi, Phys. Rev. Lett. **77**, 5047 (1996).

[7] Y. C. Lai, C. Grebogi, J. A. Yorke, and S. C. Venkataramani, Phys. Rev. Lett. **77**, 55 (1996); S. C. Venkataramani, B. Hunt, and E. Ott, Phys. Rev. E **54**, 1346 (1996); S. C. Venkataramani, B. Hunt, E. Ott, D. J. Gauthier, and J. C. Bienfang, Phys. Rev. Lett. **77**, 5361 (1996).

[8] Y. Nagai and Y.-C. Lai, Phys. Rev. E **55**, R1251 (1997).

[9] E. Ott and J. C. Sommerer, Phys. Lett. A **188**, 39 (1994).

[10] E. A. Spiegel, Ann. (N.Y.) Acad. Sci. **617**, 305 (1981); A. S. Pikovsky, Z. Phys. B **55**, 149 (1984); H. Fujisaka and T. Yamada, Prog. Theor. Phys. **74**, 919 (1985); **75**, 1087 (1986); A. S. Pikovsky and P. Grassberger, J. Phys. A **24**, 4587 (1991); A. S. Pikovsky, Phys. Lett. A **165**, 33 (1992); N. Platt, E. A. Spiegel, and C. Tresser, Phys. Rev. Lett. **70**, 279 (1993); J. F. Heagy, N. Platt, and S. M. Hammel, Phys. Rev. E **49**, 1140 (1994); Y.-C. Lai, *ibid.* **53**, R4267 (1996); **54**, 321 (1996); S. C. Venkataramani, T. M. Antonsen, Jr., E. Ott, and J. C. Sommerer, Physica D **96**, 66 (1996).

[11] Y. C. Lai, Phys. Rev. E **53**, R4267 (1996).

[12] Ashwin *et al.* have shown recently that as a system parameter changes towards the blowout bifurcation point, more and more atypical invariant measures become transversely unstable [13]. At the bifurcation, the natural measure of the chaotic attractor in **S** becomes unstable.

[13] P. Ashwin, J. Buescu, and I. N. Stewart, Phys. Lett. A **193**, 126 (1994); Nonlinearity **9**, 703 (1996); P. Ashwin, P. J. Aston, and M. Nicol, University of Surrey Technical Report, 1996 (unpublished); P. Ashwin and E. Stone, Centre for Interdisciplinary Nonlinear Mathematics Technical Report, 1997 (unpublished).

[14] Y.-C. Lai and C. Grebogi, Phys. Rev. E **52**, R3313 (1995).

[15] A. Katok, Publ. Math. IHES **51**, 377 (1980); T. Morita, H. Hata, H. Mori, T. Horita, and K. Tomita, Prog. Theor. Phys. **78**, 511 (1987); D. Auerbach, P. Cvitanović, J.-P. Eckmann, G. Gunaratne, and I. Procaccia, Phys. Rev. Lett. **58**, 2387 (1987); G. Gunaratne and I. Procaccia, *ibid.* **59**, 1377 (1987); D. Auerbach, B. O'Shaughnessy, and I. Procaccia, Phys. Rev. A **37**, 2234 (1988); P. Cvitanović and B. Eckhardt, Phys. Rev. Lett. **63**, 823 (1989); D. P. Lathrop and E. J. Kostelich, Phys. Rev. A **40**, 4028 (1989); D. Auerbach, *ibid.* **41**, 6692 (1990); D. Pierson and F. Moss, Phys. Rev. Lett. **75**, 2124 (1995); D. Christini and J. J. Collins, *ibid.* **75**, 2782 (1995); X. Pei and F. Moss, Nature (London) **379**, 619 (1996); B. Hunt and E. Ott, Phys. Rev. Lett. **76**, 2254 (1996); P. So, E. Ott, S. J. Schiff, D. T. Kaplan, T. Sauer, and C. Grebogi, *ibid.* **76**, 4705 (1996).

[16] C. Grebogi, E. Ott, and J. A. Yorke, Phys. Rev. A **36**, 3522 (1987); **37**, 1711 (1988).

[17] Y.-C. Lai, Y. Nagai, and C. Grebogi, Phys. Rev. Lett. **79**, 649 (1997).

[18] The dynamics is hyperbolic on a chaotic attractor if at each point of the trajectory the phase space can be split into an

expanding and a contracting subspace and the angle between them is bounded away from zero. Furthermore, the expanding subspace evolves into the expanding one along the trajectory and the same is true for the contracting subspace. Otherwise the set is nonhyperbolic. In general, nonhyperbolicity is a complicating feature because it can cause fundamental difficulties in the study of the chaotic systems, a known one being the shadowability of numerical trajectories by true trajectories [C. Grebogi, S. M. Hammel, and J. A. Yorke, J. Complexity **3**, 136 (1987); Bull. Am. Math. Soc. **19**, 465 (1988); C. Grebogi, S. M. Hammel, J. A. Yorke, and T. Sauer, Phys. Rev. Lett. **65**, 1527 (1990); S. Dawson, C. Grebogi, T. Sauer, and J. A. Yorke, *ibid.* **73**, 1927 (1994)].

[19] J. L. Kaplan and J. A. Yorke, in *Functional Differential Equations and Approximations of Fixed Points*, edited by H.-O. Peitgen and H.-O. Walter, Lecture Notes in Mathematics Vol. 730 (Springer, Berlin, 1979).

[20] M. Hénon, Commun. Math. Phys. **50**, 69 (1976).

[21] The mechanism leading to this scaling behavior is similar to that in the doubling transformation because the chaotic attractor in Fig. 5 is hyperbolic and its unstable direction is the y axis along which the dynamics is the doubling transformation.

[22] O. Biham and W. Wenzel, Phys. Rev. Lett. **63**, 819 (1989); Phys. Rev. A **42**, 4639 (1990).

[23] Z. You, E. J. Kostelich, and J. A. Yorke, Int. J. Bifurcation Chaos **1**, 605 (1991).

[24] A. Pikovsky and P. Grassberger, J. Phys. A **24**, 4587 (1991); A. Pikovsky, M. G. Rosenblum, and J. Kurths, Europhys. Lett. **34**, 165 (1996); M. Ding and W. Yang, Phys. Rev. E **54**, 2489 (1996).

[25] J. F. Heagy, T. L. Carroll, and L. M. Pecora, Phys. Rev. Lett. **73**, 3528 (1994).

[26] See, for example, K. T. Alligood, T. Sauer, and J. A. Yorke, *Chaos: An Introduction to Dynamical Systems* (Springer, New York, 1996).

[27] H. S. Greenside (private communication).